AGU PUBLICATIONS

JGR

Journal of Geophysical Research: Atmospheres

RESEARCH ARTICLE

10.1002/2016JD025625

Key Points:
- Important physical and quantitative differences in precipitation adjustment and feedback results arise due to computation method
- Fixed SST method provides a consistent and clear mechanistic decomposition
- Fixed SST method is less dependent on methodological choices and exhibits less variability

Supporting Information:
- Supporting Information S1

Correspondence to:
T. B. Richardson,
eetbr@leeds.ac.uk

Citation:
Richardson, T. B., B. H. Samset, T. Andrews, G. Myhre, and P. M. Forster (2016), An assessment of precipitation adjustment and feedback computation methods, *J. Geophys. Res. Atmos.*, *121*, doi:10.1002/2016JD025625.

Received 11 JUL 2016
Accepted 26 SEP 2016
Accepted article online 28 SEP 2016

An assessment of precipitation adjustment and feedback computation methods

T. B. Richardson[1], B. H. Samset[2], T. Andrews[3], G. Myhre[2], and P. M. Forster[1]

[1]School of Earth and Environment, University of Leeds, Leeds, UK, [2]Center for International Climate and Environmental Research, Oslo, Norway, [3]Met Office Hadley Centre, Exeter, UK

Abstract The precipitation adjustment and feedback framework is a useful tool for understanding global and regional precipitation changes. However, there is no definitive method for making the decomposition. In this study we highlight important differences which arise in results due to methodological choices. The responses to five different forcing agents (CO_2, CH_4, SO_4, black carbon, and solar insolation) are analyzed using global climate model simulations. Three decomposition methods are compared: using fixed sea surface temperature experiments (fSST), regressing transient climate change after an abrupt forcing (regression), and separating based on timescale using the first year of coupled simulations (YR1). The YR1 method is found to incorporate significant SST-driven feedbacks into the adjustment and is therefore not suitable for making the decomposition. Globally, the regression and fSST methods produce generally consistent results; however, the regression values are dependent on the number of years analyzed and have considerably larger uncertainties. Regionally, there are substantial differences between methods. The pattern of change calculated using regression reverses sign in many regions as the number of years analyzed increases. This makes it difficult to establish what effects are included in the decomposition. The fSST method provides a more clear-cut separation in terms of what physical drivers are included in each component. The fSST results are less affected by methodological choices and exhibit much less variability. We find that the precipitation adjustment is weakly affected by the choice of SST climatology.

1. Introduction

Global mean precipitation is tightly constrained by the tropospheric energy budget, whereby the latent heat released from precipitation balances tropospheric cooling [*Mitchell*, 1983; *Allen and Ingram*, 2002; *O'Gorman et al.*, 2011; *Pendergrass and Hartmann*, 2014]. As a result, the change in global mean precipitation in response to forcing can be decomposed into a rapid adjustment and feedback response. The adjustment is due to direct changes in atmospheric cooling in response to the forcing and any associated rapid adjustments in the climate system which affect the atmospheric energy budget, such as rapid changes in atmospheric temperature, water vapor, and clouds [*Lambert and Faull*, 2007; *Bala et al.*, 2009; *Andrews et al.*, 2010]. The feedback response is driven by surface temperature-dependent radiative feedbacks [*Previdi*, 2010]. The decomposition is highly useful for understanding the different hydrological responses to different forcing agents [*Andrews et al.*, 2010; *Cao et al.*, 2011; *Kravitz et al.*, 2013; *Kvalevåg et al.*, 2013; *Fläschner et al.*, 2016; *Samset et al.*, 2016]. The simple energetically constrained adjustment and feedback model can be used to accurately emulate historical and 21st century global mean precipitation changes predicted by general circulation models [*Thorpe and Andrews*, 2014]. A recent study [*Cao et al.*, 2015] found that the linear combination of adjustment and feedback can be used to emulate precipitation change predicted by climate models under different CO_2 and solar forcing scenarios.

One problem with the adjustment and feedback framework is that there is no definitive method for making the decomposition. There are a range of methods which can be used to calculate the precipitation adjustment and feedback components. These include using fixed sea surface temperature (SST) experiments [*Bala et al.*, 2009; *Andrews et al.*, 2010; *Richardson et al.*, 2016; *Samset et al.*, 2016; *Tian et al.*, 2016], linear regression of precipitation change against surface temperature change [*Lambert and Faull*, 2007; *Andrews et al.*, 2009], or separating based on timescale [*Cao et al.*, 2012; *Bony et al.*, 2013]. However, these different methods result in subtly different adjustment and feedback definitions. It is not well understood how the results and uncertainties vary between methods. It is important to understand the effects of different methodological choices on the adjustment and feedback framework and how they relate to physical understanding.

On regional scales the decomposition becomes more complicated as local precipitation is strongly influenced by circulation changes [*Bony et al*., 2013; *Chadwick et al*., 2013; *Huang*, 2013; *Richardson et al*., 2016]. As a result any surface temperature change which may be included in the rapid adjustment calculation can strongly affect the spatial pattern of precipitation change [*Chadwick et al*., 2014; *Richardson et al*., 2016]. This makes the regional decomposition nontrivial, and careful consideration is required for methodology. In this study we compare methods for calculating adjustment and feedback precipitation responses to five different forcing scenarios, on global and regional scales using two global climate models.

2. Methods

2.1. Adjustment and Feedback Calculation

Three different methodologies are analyzed for decomposing the precipitation adjustment and feedback terms in response to forcing: using fixed sea surface temperature experiments (fSST), separating based on timescale (YR1), and linear regression during transient climate change (regression). The decomposition is used to aid physical understanding, and there is no true value with which to compare. In this study we compare how the different methods affect the physical interpretation of results and assess their usefulness based on error characteristics and consistency.

2.1.1. fSST Method

The adjustment component can be estimated using fixed sea surface temperature experiments (fSST) [*Bala et al*., 2009; *Andrews et al*., 2010]. In these simulations the fixed SST inhibits oceanic temperature-dependent feedbacks, thus isolating the adjustment component. Land surface temperatures can change, which will influence the precipitation adjustment. The feedback response (ΔP_{fb}) is calculated by subtracting the fixed SST precipitation change (ΔP_{ra}) from the total response in fully coupled simulations (ΔP_{tot}). The hydrological sensitivity (precipitation feedback per unit kelvin) is calculated by dividing the feedback response by global mean surface temperature change, as shown in equation (1). It should be noted that this differs from the apparent hydrological sensitivity [*Fläschner et al*., 2016; *Samset et al*., 2016] which is the total precipitation response per unit kelvin.

$$\mathrm{HS} = \frac{\Delta P_{\mathrm{fb}}}{\Delta T_{\mathrm{tot}} - \Delta T_{\mathrm{ra}}} = \frac{\Delta P_{\mathrm{tot}} - \Delta P_{\mathrm{ra}}}{\Delta T_{\mathrm{tot}} - \Delta T_{\mathrm{ra}}} \tag{1}$$

where HS is the hydrological sensitivity, ΔP_{fb} is the precipitation feedback response, ΔP_{tot} is the total precipitation response, ΔP_{ra} is the precipitation adjustment, ΔT_{tot} is the total surface temperature response, and ΔT_{ra} is any surface temperature change included in the adjustment calculation. Fully coupled climate models can take millennia to reach true equilibrium after large step forcings [*Caldeira and Myhrvold*, 2013]; however, this is not necessary for calculating the precipitation feedback per unit temperature change (hydrological sensitivity). For slab ocean model simulations, as used for CESM1-CAM4, a shorter time period is required to reach a new equilibrium (several decades). Here the total precipitation/temperature response is taken as the mean change 50 years after introducing a forcing, by which time significant temperature change has occurred. In our uncertainty analysis the meaning period is adjusted in length along with the fSST integration length.

2.1.2. Regression Method

The adjustment and hydrological sensitivity can also be estimated through linear regression during transient climate change [*Gregory and Webb*, 2008; *Andrews et al*., 2009], hereafter denoted as the "regression" method. By regressing precipitation change against global mean surface temperature change after an abrupt forcing, the adjustment is given by the intercept and the hydrological sensitivity obtained from the slope. This methodology implies that no global mean surface temperature effects are included in the adjustment component. However, it has been noted that rapid SST change can produce a spatial pattern with zero global mean but which still affects the atmospheric energy budget [*Andrews et al*., 2015]. This method has typically only been used for global mean analysis; however, we will also assess the suitability of regression for local precipitation. The local precipitation at each grid point is regressed against the global mean temperature change to calculate the regional adjustment and hydrological sensitivity.

2.1.3. YR1 Method

The precipitation response to forcing can also be separated based on timescale [*Cao et al*., 2012; *Bony et al*., 2013], defining the adjustment as any changes which occur within a designated time period after a forcing is applied. Following *Bony et al*. [2013], we take the first year precipitation response as the adjustment, hereafter denoted as the "YR1" method. Using this method, any change in precipitation which occurs within 1 year of an abrupt forcing is included. Consequently, some changes in precipitation driven by surface temperature change are included in the adjustment component, as both land and sea surface temperatures are free to change. The feedback response can be calculated by subtracting the first year response (ΔP_{ra}) from the total response (ΔP_{tot}). The total response is calculated using the mean change in precipitation for years 51–70 in the abrupt forcing coupled simulations. The hydrological sensitivity is then calculated by dividing the feedback response by surface temperature change, as shown in equation (1).

2.2. Simulations

We analyze simulations from the Precipitation Driver Response Model Intercomparison Project (PDRMIP) [*Samset et al.*, 2016]. The uncertainty analysis focuses on output from HadGEM2 [*Martin et al.*, 2011] and CESM1-CAM4 [*Neale et al.*, 2010; *Gent et al.*, 2011] for which extended runs were performed. Data from nine PDRMIP models (CanESM2, GISS-E2-R, HadGEM2, HadGEM3, MPI-ESM, CESM1-CAM4, CESM1-CAM5, NorESM1, and MIROC-SPRINTARS) are used for an overall comparison of the three methods (Figure 3). For details on PDRMIP protocols, see *Samset et al.* [2016]. Five different abrupt forcing scenarios were implemented: a doubling of CO_2 concentration (2xCO2), tripling of CH_4 concentration (3xCH4), 2% increase in solar insolation (SOL), 5 times SO_4 concentration or emissions (5xSO4), and 10 times black carbon concentration or emissions (10xBC).

HadGEM2 and CESM1 implemented the scenarios with some differences, so responses would not be expected to be quantitatively similar. HadGEM2 used a preindustrial baseline for all simulations, whereas CESM1 used a present-day baseline. For the aerosol experiments HadGEM2 scaled emissions, whereas CESM1 scaled concentrations based on AeroCom Phase II [see, e.g., *Samset et al.*, 2013]. In addition, HadGEM2 employed a fully coupled ocean model, whereas CESM1 used a slab-ocean model. All simulations were performed both with sea surface temperatures held fixed (fSST) and coupled to an ocean. The fSST simulations were run for 30 years and the coupled runs for 100 years. Five 20 year coupled 2xCO2 ensemble runs were also performed in CESM1.

An additional set of simulations were performed using HadGEM2 to investigate the effect of SST climatology on the precipitation adjustment. Two fixed SST simulations with CO_2 levels quadrupled were run for 20 years, one with preindustrial SST climatology (sstClim4xCO2) and one with a uniform increase of 4 K from preindustrial SST climatology (sstClim4K4xCO2). Corresponding baseline simulations were run for the two SST climatologies, denoted sstClim and sstClim4K, respectively. The precipitation adjustment was calculated as the difference between the forced run and corresponding control run averaged across the full 20 years.

2.3. Error Calculations

The standard error for the precipitation adjustment and hydrological sensitivity is computed to compare methods. For fSST simulations equation (2) is used to calculate the standard error (SE), where "σ" is the standard deviation of the annual mean anomaly and "n" is the length (in years) of the run:

$$\mathrm{SE} = \frac{\sigma}{\sqrt{n}} \tag{2}$$

Because the coupled runs have not reached true equilibrium, there is still a temperature-dependent trend in the precipitation response. Therefore, the standard deviation (σ) is computed based solely on the control run. The annual mean standard deviation of the control run is multiplied by the square root of 2 to account for the fact that the precipitation response is the difference between two means.

The standard error for the regression adjustment ($\mathrm{SE_{ra}}$) is taken as the standard error of the intercept using equation (3) and the standard error of the hydrological sensitivity ($\mathrm{SE_{hs}}$) taken as the standard error of the slope using equation (4):

$$\mathrm{SE_{ra}} = \sqrt{\frac{\Sigma {x_i}^2 \Sigma (y_i - \overline{y_i})^2}{n(n-2)\Sigma (x_i - \overline{x_i})^2}} \tag{3}$$

$$\mathrm{SE_{hs}} = \sqrt{\frac{\Sigma (y_i - \overline{y_i})^2}{(n-2)\Sigma (x_i - \overline{x_i})^2}} \tag{4}$$

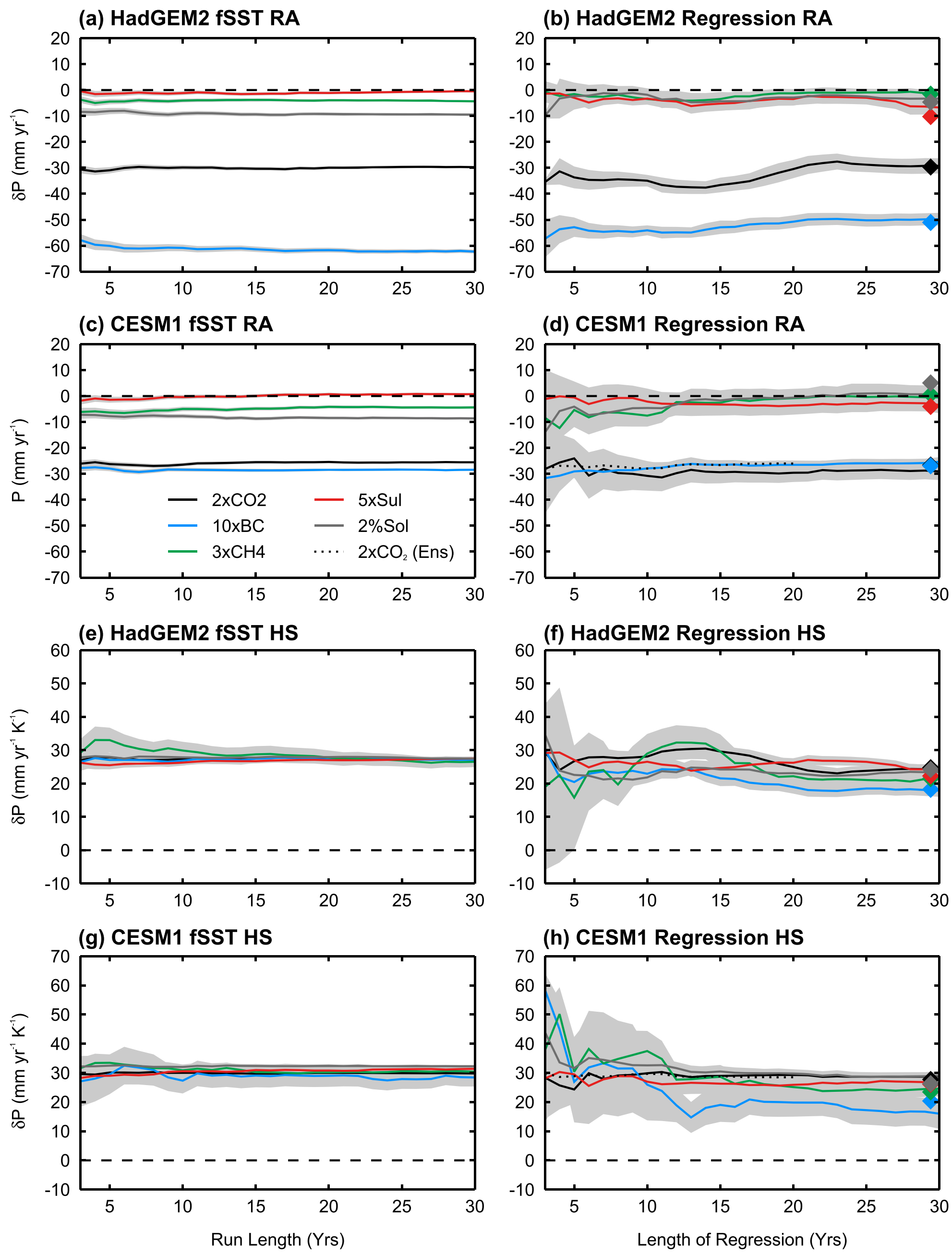

Figure 1. Global mean rapid adjustment (RA) and hydrological sensitivity (HS) terms against integration length for (a, c, e, and g) fSST and (b, d, f, and h) regression methods. Results are shown for the five forcing scenarios (colored lines) implemented in HadGEM2 and CESM1. Also shown in the CESM1 regression plots are RA and HS values obtained from regression of five 2xCO_2 ensemble members (dotted line). The grey shading denotes the standard error. Diamonds indicate regression values after 100 years.

where x_i is temperature change each year, y_i is precipitation change each year, n is the number of years regressing over, and overbars denote the average value of that quantity.

3. Results and Discussion

3.1. Global Mean Method Comparison

The choice of integration length and regression length impacts on both the adjustment and hydrological sensitivity results and their error characteristics. Figure 1 shows how the precipitation adjustment and

Table 1. Hydrological Sensitivity Calculated Using Regression Technique Over Years 1–10 and 11–100 of Abrupt Forcing Simulations for HadGEM2 and CESM1-CAM4[a]

	HadGEM2		CESM1-CAM4	
	Years 1–10	Years 11–100	Years 1–10	Years 11–100
2xCO2	28.1 ± 1.5	22.9 ± 1.5	29.9 ± 2.7	22.7 ± 2.9
3xCH4	29.0 ± 5.9	21.4 ± 1.9	37.5 ± 6.9	18.4 ± 4.2
5xSul	26.5 ± 1.6	19.5 ± 1.5	27.0 ± 4.4	19.9 ± 4.5
10xBC	23.0 ± 1.9	20.1 ± 2.6	26.0 ± 12.3	20.0 ± 4.0
SOL	21.8 ± 1.7	24.5 ± 2.1	32.6 ± 2.6	19.2 ± 3.9

[a]Uncertainty values are the standard error of the regression slope.

hydrological sensitivity vary with changing integration/regression length. For all forcing scenarios the fSST precipitation adjustment is very consistent irrespective of the number of years analyzed (Figures 1a and 1c). Integration length has a larger effect on the fSST hydrological sensitivity (Figures 1e and 1g) in response to 3xCH4 and 10xBC. This is likely because these forcing scenarios drive smaller temperature changes (see Figure 4), thus resulting in larger errors per unit kelvin. There is also more natural variability associated with the hydrological sensitivity calculation, arising from the coupled ocean. The variation in the fSST hydrological sensitivity is small for all forcing scenarios when using over 15 years for the calculation.

Regression length has a much larger impact on the adjustment and hydrological sensitivity (Figures 1b, 1d, 1f, and 1h). Particularly with a regression length less than 15 years, the adjustment and hydrological sensitivity vary considerably dependent on the number of years analyzed. Using a five-member ensemble for regression reduces the variability (Figures 1d and 1h dotted line). The hydrological sensitivity generally reduces as regression length increases (Figures 1f and 1h), particularly for CESM1. It has previously been shown that top of the atmosphere energy budget feedbacks are not constant in many models following abrupt forcings [*Andrews et al.*, 2012]. The changing hydrological sensitivity with regression length implies that net atmospheric energy budget feedbacks are also not constant throughout the abrupt forcing simulations. Table 1 shows the hydrological sensitivity calculated separately using the first 10 years and the following 90 years of the simulations. For both models the hydrological sensitivity is generally larger when computed using the first 10 years. This slight nonlinearity means that methodological choices will affect results. As a consequence, it should be noted that using a longer regression to improve statistics (as shown in Figure 2) may not be beneficial for capturing the initial adjustment component.

Increasing the integration length and regression length reduces the adjustment and hydrological sensitivity uncertainties (Figure 2). Across most forcing agents a standard error of less than 1 mm yr^{-1} for the fSST adjustment can be obtained with a minimum integration length of 8 years. The only exception is 10xBC for HadGEM2 which exhibits a slightly larger variability than the other scenarios. Using the regression method, it is not possible to constrain the adjustment response to within 1 mm yr^{-1}, even after 100 years, for any forcing scenario. Using five 20 year ensemble members, regression still fails to constrain the adjustment to within 1 mm yr^{-1} (Figure 2d). The fSST adjustment error is not strongly affected by forcing scenario, whereas the regression adjustment error is generally larger for stronger forcings. The YR1 adjustment uncertainty is large due to the short time period (4.6 mm yr^{-1} and 4.7 mm yr^{-1} for HadGEM2 and CESM1, respectively). Multiple ensemble members could be used to reduce this uncertainty.

For the hydrological sensitivity regression errors are again larger than the fSST errors; however, the difference is smaller. Errors in the hydrological sensitivity for both methods are strongly influenced by the magnitude of surface temperature change. Forcing scenarios which produce more surface temperature change in the coupled runs (see Figure 4) have smaller errors in the hydrological sensitivity. The use of a five-member ensemble for regression reduces the hydrological sensitivity uncertainty, and a standard error of less than 1 mm yr^{-1} can be achieved using 10 years (Figure 2h).

Figure 3 shows the PDRMIP multimodel mean precipitation adjustment and hydrological sensitivity calculated using the fSST, regression, and YR1 methods diagnosed using an integration/regression length of 15 years. Across the forcing scenarios the fSST and regression precipitation adjustments (Figures 3a and 3b) are generally in close agreement. The YR1 adjustments show more disagreement, particularly in response to 2xCO2 and 5xSul. This is due to the influence of temperature-dependent feedbacks occurring in the first year of coupled simulations. In particular, significant surface temperature change occurs in the first year of the 2xCO2, 5xSO4, and SOL simulations (Figure 4), which have the largest radiative forcings of the five

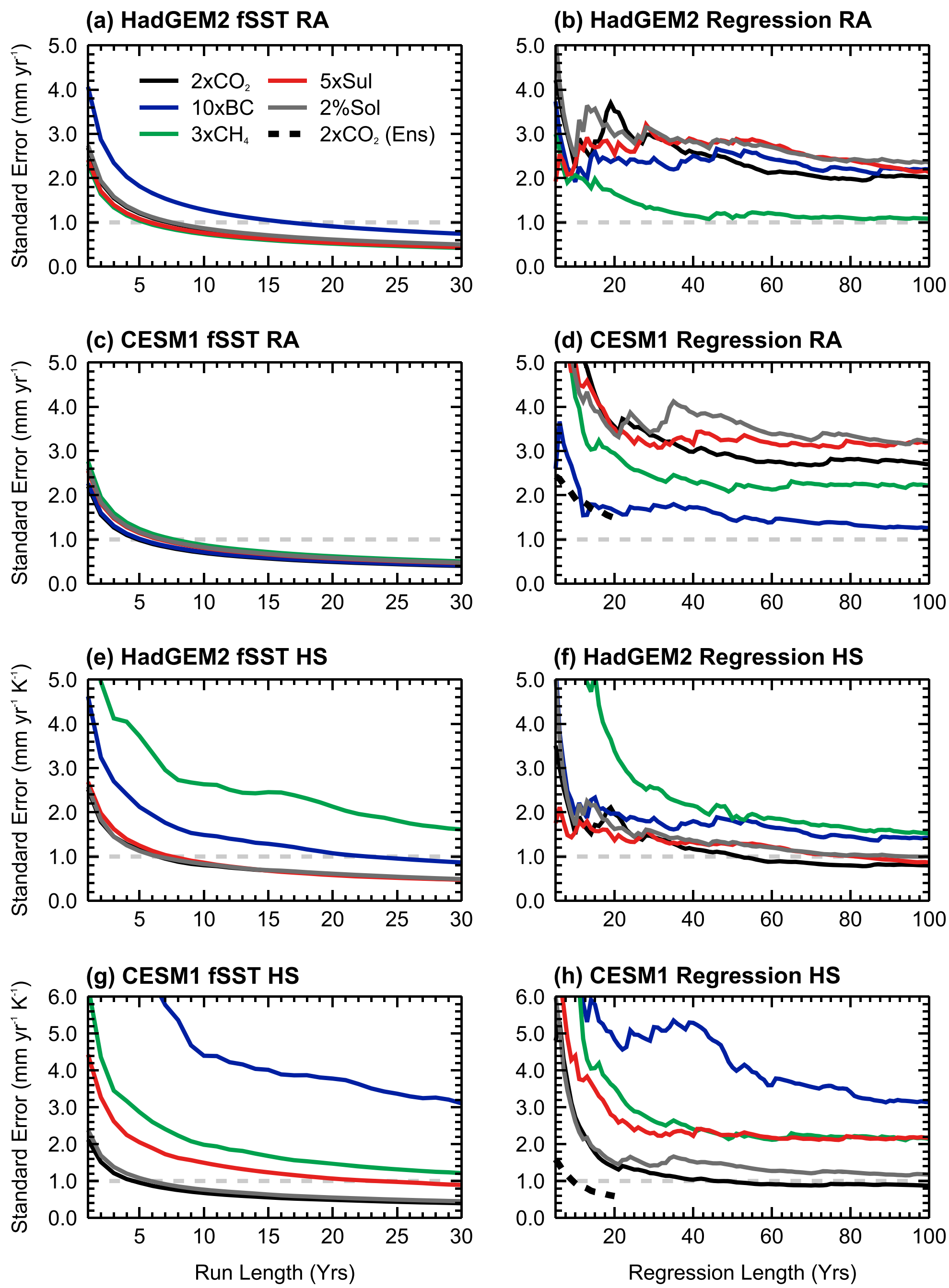

Figure 2. Standard error of global mean rapid adjustment (RA) and hydrological sensitivity (HS) values against integration length for (a, c, e, and g) fSST and (b, d, f, and h) regression methods. Results are shown for the five different forcing scenarios (colored lines) implemented for HadGEM2 and CESM1. The dotted line in CESM1 regression plots shows the RA and HS standard error computed using five 2xCO2 ensemble members.

scenarios. Some surface temperature change also occurs in the fSST experiments, but it is much smaller in magnitude. In addition, accounting for the fSST surface temperature change generally does not bring the adjustment value into better agreement with the alternate methods, also discussed in *Samset et al*. [2016]. Similar findings have been shown in previous studies for top of the atmosphere effective radiative forcing calculated using fSST methods [*Hansen et al*., 2005; *Sherwood et al*., 2015]. Using a shorter time period, such as 1 month, to calculate the adjustment reduces the incorporation of temperature-dependent effects.

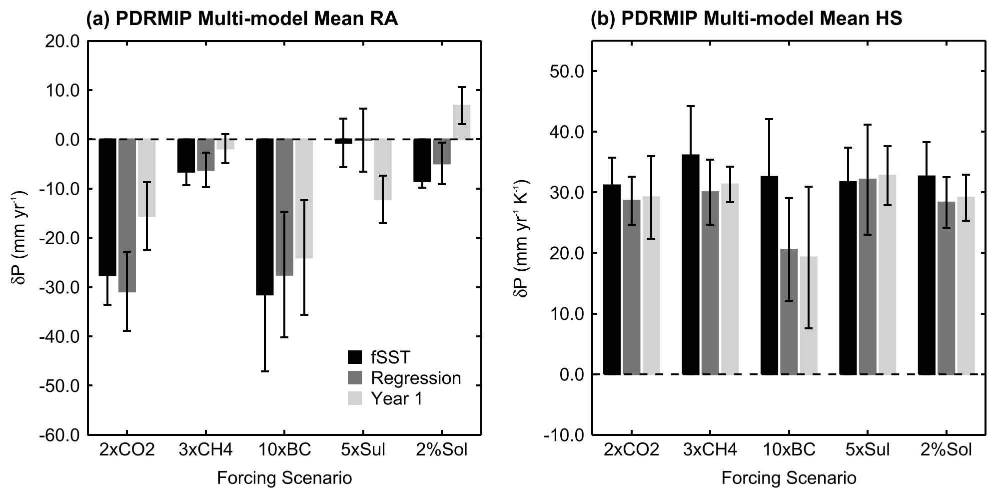

Figure 3. PDRMIP multimodel global mean rapid adjustment (RA) and hydrological sensitivity (HS) values across forcing scenarios diagnosed using fSST, regression, and YR1 methods. A run and regression length of 15 years is utilized. Error bars denote the standard deviation of the model spread.

However, the uncertainty becomes very large due to monthly natural variability, and the results differ greatly from the other methods (see supporting information Table S1).

The hydrological sensitivity (Figures 3c and 3d) is mostly consistent between the three methodologies across forcing scenarios, but there are some noteworthy differences. The fSST method gives a systematically larger sensitivity, but the methods generally agree within their uncertainties. There is a notable difference between the 10xBC hydrological sensitivity calculated using fSST and the other methods. The fSST hydrological sensitivity is very consistent with other forcing scenarios, whereas the regression and YR1 values for 10xBC are somewhat lower. The precipitation response to black carbon does not scale as well with surface temperature change in the first few years after introducing a forcing, as seen from the varying hydrological sensitivity with regression length in Figures 1f and 1h. This could lead to discrepancies between decomposition methods. *Rugenstein et al.* [2016] found that shortwave cloud radiative effects in response to forcing do not scale well with surface temperature and are, in fact, driven by ocean-atmosphere adjustments with a characteristic timescale of a few years. Black carbon strongly affects atmospheric shortwave cooling, and it can be seen that the difference between methods arises mainly from the top of the atmosphere shortwave feedback (see supporting information Figure S7). It should be noted that ocean-driven effects on adjustments will not be included in the fSST adjustment results. For the regression method it is unclear how potential ocean adjustments would be partitioned as they occur over multiple years and do not scale with global surface temperature change.

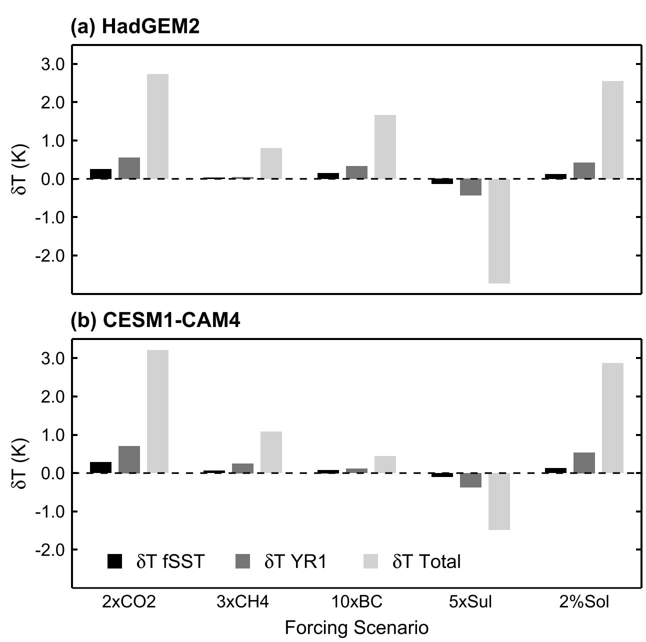

Figure 4. Global mean surface temperature change (δT) in response to the five forcing scenarios for the fSST simulations (averaged over full 30 years), first year of coupled simulations (YR1), and final 50 years of coupled simulations (Total). Results are shown for (a) HadGEM2 and (b) CESM1-CAM4.

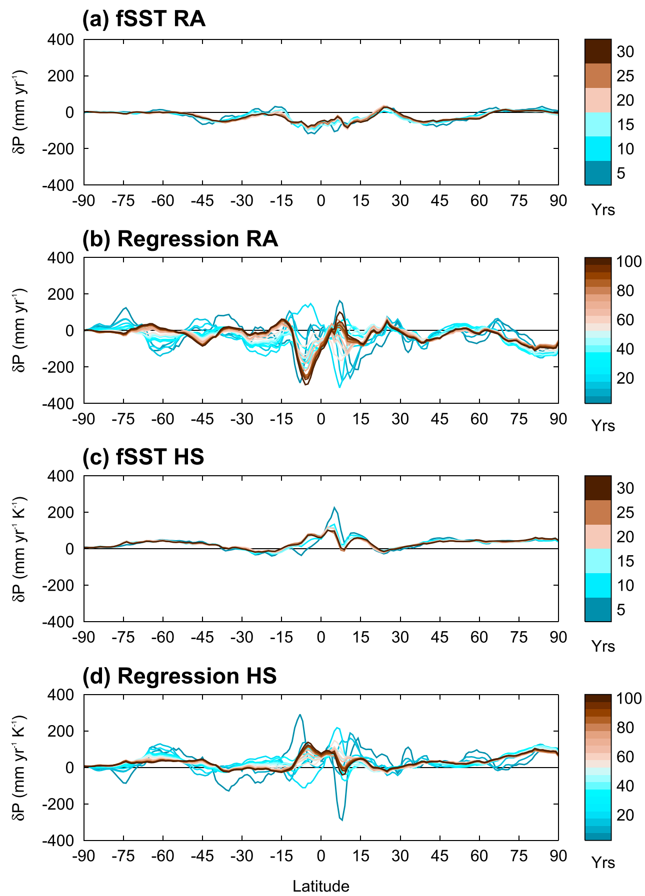

Figure 5. HadGEM2 zonally averaged precipitation adjustment (RA) and hydrological sensitivity (HS) in response to 2xCO2 calculated using (a, c) fSST and (b, d) regression methods. Each shaded line shows the response calculated using an integration/regression length increasing incrementally by 5 years.

3.2. Regional Method Comparison

Figure 5 shows how integration/regression length affects the zonal mean precipitation adjustment and hydrological sensitivity in response to doubling CO_2 for HadGEM2. It can be seen that the fSST zonal mean adjustment and hydrological sensitivity are fairly independent of integration length, with only small variations within the tropics. In contrast, the adjustment and sensitivity calculated using regression are highly dependent on the number of years analyzed. Particularly for the adjustment component, in many regions the response is completely reversed as the regression length increases. This is likely because local shifts in precipitation patterns may not scale well with global mean temperature change and therefore lead to erroneous regression results. This makes the choice of regression length very difficult, as increasing the number of years will improve statistics, but may not give a good representation of the initial adjustment. Similar results are seen for CESM1 and the other forcing scenarios (see supporting information Figures S1–S3).

A comparison of the 2xCO2 regional adjustment and hydrological sensitivity calculated using the three methodologies for CESM1-CAM4 is shown in Figure 6 (for 5xSul and HadGEM2 responses, see supporting information Figures S4–S6). An integration/regression length of 20 years is used for the calculations. The spatial pattern of the adjustment and hydrological sensitivity exhibit significant differences between methods, particularly for the adjustment component. In many regions the methods disagree substantially on the magnitude and sign of precipitation changes. Even the zonally averaged responses exhibit large differences, particularly in the tropics. The regression and YR1 responses have large uncertainties; over most of the globe the signal is smaller than the standard error (stippling denotes where signal is greater than the standard error), particularly for the adjustment component. In contrast, in most regions where large changes occur using the fSST method, the signal is larger than the standard error.

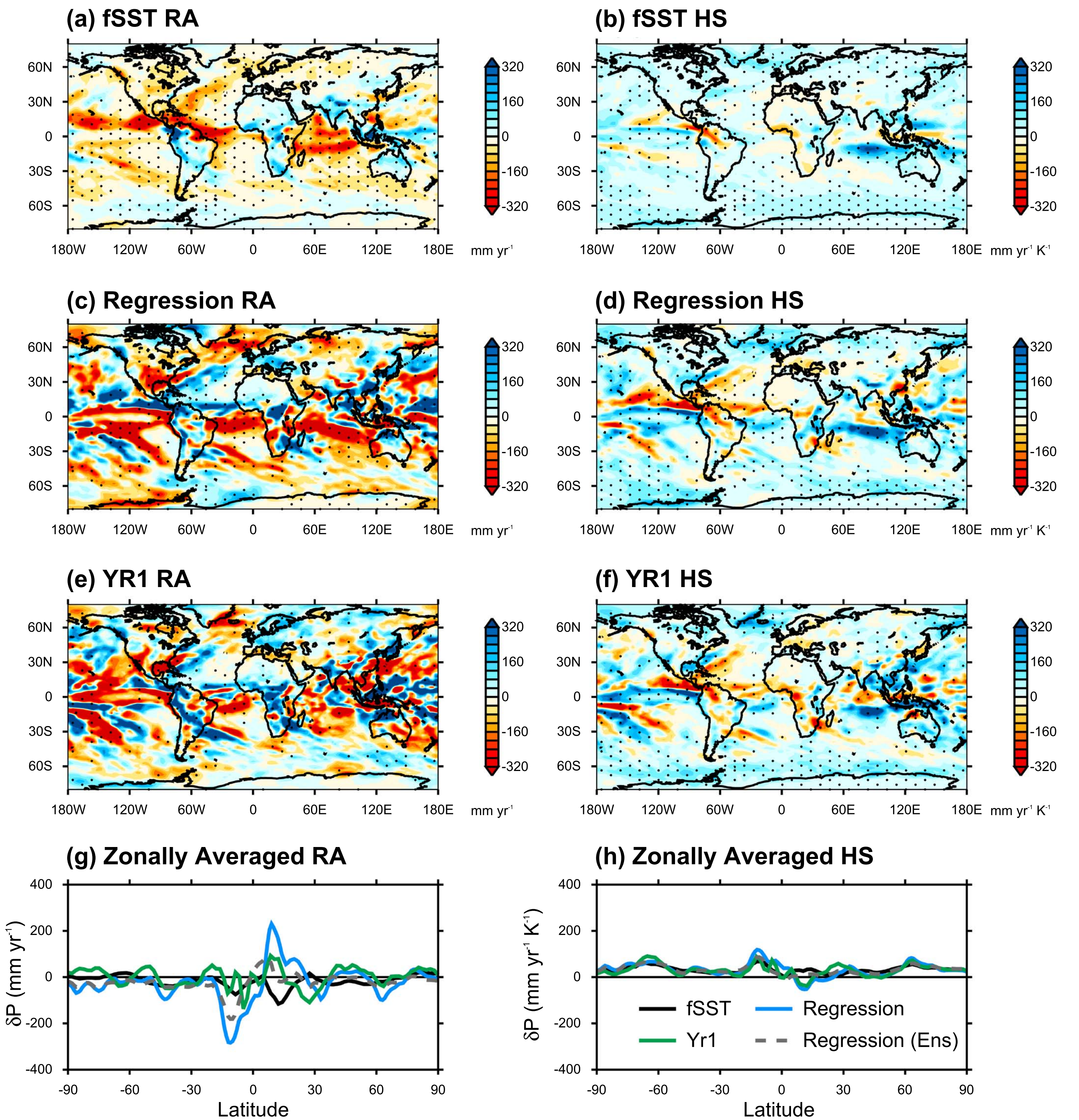

Figure 6. CESM1-CAM4 regional (a, c, e, and g) precipitation adjustment (RA) and (b, d, f, and h) hydrological sensitivity (HS) response to doubling CO_2 calculated using fSST (Figures 6a and 6b), regression (Figures 6c and 6d), and YR1 (Figures 6e and 6f) methods. Figures 6g and 6h show the zonally averaged response for all three methods. Stippling shows where the signal is greater than the standard error. An integration/regression length of 20 years is used to compute the responses.

The hydrological sensitivity shows slightly more agreement between methods, especially in the midlatitudes. This is likely because precipitation change is mainly thermodynamically driven in the midlatitudes [*Emori*, 2005; *Seager et al.*, 2010] and follows global mean temperature change well. In the tropics, however, where dynamic changes play a key role [*Chou et al.*, 2009; *Bony et al.*, 2013], large differences arise. Given that these

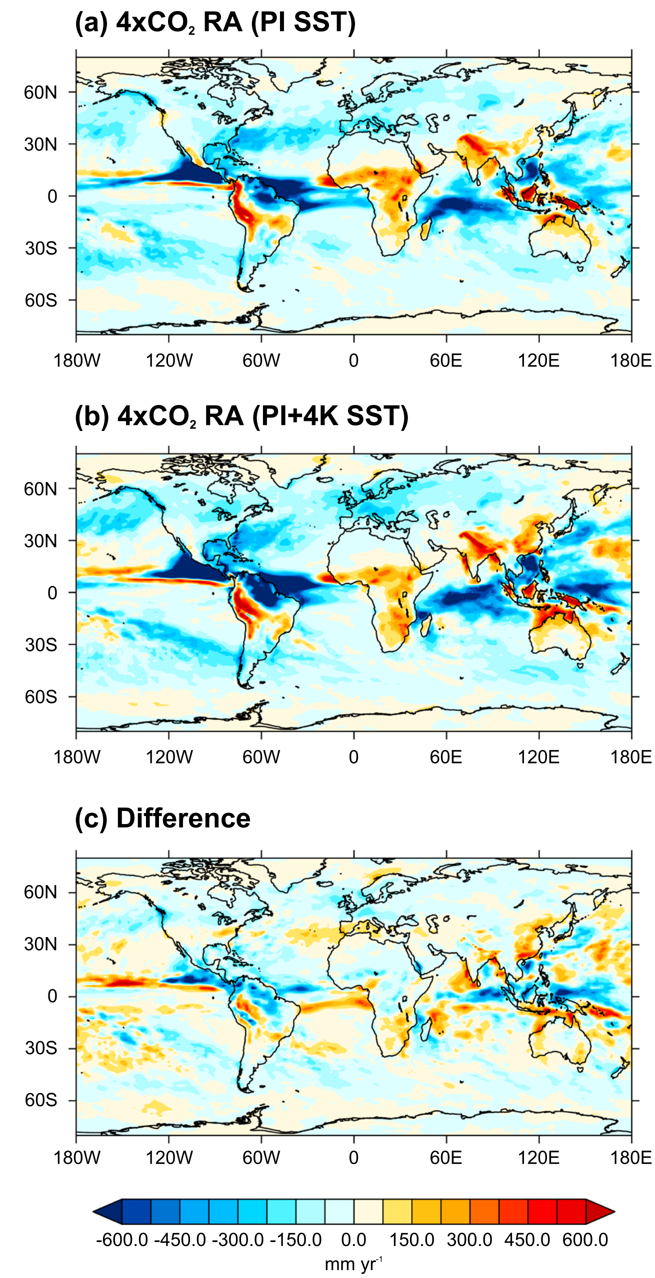

Figure 7. HadGEM2 precipitation adjustment in response to quadrupling CO_2 calculated using fixed SST simulations with (a) preindustrial SST climatology, (b) preindustrial plus 4 K SST climatology, and (c) the difference between the two.

dynamic changes do not necessarily scale well with global mean temperature change, regional regression may not yield useful information within the adjustment and feedback framework. It can be seen in Figure 6 that the pattern of adjustment and hydrological sensitivity using regression tend to be similar but opposite in sign in the tropics. This could be indicative of a statistical artifact arising due to the regression methodology, rather than a physically meaningful result.

The fSST method provides a more clear-cut decomposition in terms of which drivers are included in the precipitation adjustment and feedback components regionally. Within the fSST simulations, only the direct impact of the forcing agent on the troposphere and the effects of land surface temperature change are included. This enables a better mechanistic understanding of what processes drive precipitation change. The YR1 method incorporates significant global surface temperature change over both land and sea into the adjustment and therefore is not a useful tool in separating drivers of precipitation change. The huge variation in regression results as the number of years analyzed changes makes it difficult to understand what effects are being included. In addition, it has previously been noted that rapid SST adjustment in response to CO_2 can produce a spatial pattern of surface temperature change, but with zero global mean [*Andrews et al.*, 2015]. These local SST changes may impact the local precipitation adjustment.

3.3. SST Climatology

Another methodological choice which must be considered is the base state climatology. To investigate the effect of different sea surface temperature (SST) climatologies, we analyze the precipitation response to quadrupling CO_2 with preindustrial SST climatology, and preindustrial plus 4 K SST climatology, using HadGEM2 as outlined in section 2.2. Globally, there is a small difference in precipitation adjustments, with a reduction of -65.0 ± 0.5 mm yr^{-1} and -73.3 ± 0.6 mm yr^{-1} for sstClim4xCO2 and sstClim4K4xCO2, respectively. The difference arises mainly due to the change in longwave cooling of the troposphere (see supporting information Figure S8). In the warmer climate the upwelling longwave radiation at the surface and top of the atmosphere are increased, and the atmospheric temperature and humidity profiles altered. As a result, an equivalent increase in CO_2 concentration produces a larger reduction in longwave cooling from the atmosphere. Although there is a significant difference in the absolute precipitation response, the percentage change in precipitation is in close agreement, with changes of $-5.77 \pm 0.04\%$ and $-5.82 \pm 0.05\%$.

Figure 7 shows the regional precipitation adjustment for the two experiments and difference between the two. The spatial pattern of the precipitation response is largely unaffected by the different SST climatologies. There are locally some larger differences in precipitation change within the tropics, due to small shifts in the pattern of change resulting from the different SST climatologies. If the spatial pattern of SST climatology was significantly altered, this may have a larger effect on the regional adjustment.

4. Conclusions

The adjustment and feedback framework is a useful tool for understanding global and regional precipitation changes. However, it has been highlighted here that important differences arise in results based upon the decomposition method employed, which are important to understand and consider. Globally, the precipitation adjustment and hydrological sensitivity calculated using fSST and regression methods are generally in good agreement. However, the regression values can vary considerably when using a short regression length (less than ~20 years). In addition, the fSST method gives a systematically larger and more consistent hydrological sensitivity. The YR1 method exhibits significant differences to the other methods, particularly in response to doubling CO_2. This is due to the substantial surface temperature change which occurs within the first year of coupled simulations. The YR1 method is therefore not a very useful tool for making the adjustment and feedback decomposition. Using a shorter timescale, such as 1 month, considerably increases the uncertainty.

The uncertainties associated with the regression method are much larger than for fSST. To an extent this can be improved through the use of ensembles; however, the regression errors for the adjustment in response to 2xCO2 are still larger with a five-member ensemble. Increasing integration and regression length improves the error characteristics for both fSST and regression methods. Using a fSST integration length of at least 8 years reduces the standard error for the global mean precipitation adjustment to under 1 mm yr^{-1}. The errors are larger for the hydrological sensitivity, and a longer integration is recommended.

Regionally, significant differences arise between methods. Using regression, the adjustment and hydrological sensitivity are highly dependent on regression length, with the pattern of change completely reversing in many regions as the number of years increases. This makes it difficult to understand what effects are being represented in the regression decomposition. In contrast, the fSST method gives a consistent spatial pattern of adjustment and hydrological sensitivity irrespective of integration length. The YR1 response includes a high level of noise and is influenced by rapid SST changes within the first year. There is better agreement between methods for the hydrological sensitivity in the midlatitudes, where the precipitation response is thermodynamically driven, scaling well with global mean temperature change.

The choice of SST climatology has a weak effect on the absolute precipitation adjustment. An increase in SST of 4 K increases the magnitude of the global mean precipitation adjustment from -65.0 ± 0.5 mm yr^{-1} to -73.3 ± 0.6 mm yr^{-1}. However, the percentage change in precipitation from the control state is in close agreement despite the different SST climatologies. The spatial pattern of precipitation adjustment is largely unaffected by a warmer SST climatology. Locally, in the tropics there are some differences in precipitation change due to small shifts in the pattern of change.

Based on these results, we find that the fSST method provides a more clearly defined separation. The adjustment term includes the direct impact of a forcing agent on the troposphere and the effects of land surface temperature change. The feedback term includes any effects mediated by SST change. The fSST method is less affected by methodological choices and exhibits much less variability. An integration length of at least 15 years is recommended to reduce uncertainties, particularly for regional analysis.

Acknowledgments
The PDRMIP model output is all publicly available; for data access, visit http://www.cicero.uio.no/en/PDRMIP/PDRMIP-data-access. T.R. was supported by a NERC CASE award in collaboration with the Met Office NE/K007483/1. HadGEM2 simulations were performed using the MONSooN system, a collaborative facility supplied under the Joint Weather and Climate Research Programme, which is a strategic partnership between the Met Office and the Natural Environment Research council. P.M.F. was supported by a Royal Society Wolfson Merit Award and NERC grant NE/K006038/1. T.A. was supported by the Joint UK BEIS/Defra Met Office Hadley Centre Climate Programme (GA01101). B.H.S. and G.M. were funded by the Research Council of Norway, through the grant NAPEX (229778). Supercomputer facilities were provided by NOTUR.

References

Allen, M. R., and W. J. Ingram (2002), Constraints on future changes in climate and the hydrologic cycle, *Nature*, *419*, 224–232, doi:10.1038/nature01092.

Andrews, T., P. M. Forster, and J. M. Gregory (2009), A surface energy perspective on climate change, *J. Clim.*, *22*(10), 2557–2570, doi:10.1175/2008JCLI2759.1.

Andrews, T., P. M. Forster, O. Boucher, N. Bellouin, and A. Jones (2010), Precipitation, radiative forcing and global temperature change, *Geophys. Res. Lett.*, *37*, L14701, doi:10.1029/2010GL043991.

Andrews, T., J. M. Gregory, M. J. Webb, and K. E. Taylor (2012), Forcing, feedbacks and climate sensitivity in CMIP5 coupled atmosphere-ocean climate models, *Geophys. Res. Lett.*, *39*, L09712, doi:10.1029/2012GL051607.

Andrews, T., J. M. Gregory, and M. J. Webb (2015), The dependence of radiative forcing and feedback on evolving patterns of surface temperature change in climate models, *J. Clim.*, *28*(4), 1630–1648, doi:10.1175/JCLI-D-14-00545.1.

Bala, G., K. Caldeira, and R. Nemani (2009), Fast versus slow response in climate change: Implications for the global hydrological cycle, *Clim. Dyn.*, *35*(2–3), 423–434, doi:10.1007/s00382-009-0583-y.

Bony, S., G. Bellon, D. Klocke, S. Sherwood, S. Fermepin, and S. Denvil (2013), Robust direct effect of carbon dioxide on tropical circulation and regional precipitation, *Nat. Geosci.*, *6*(6), 447–451, doi:10.1038/ngeo1799.

Caldeira, K., and N. P. Myhrvold (2013), Projections of the pace of warming following an abrupt increase in atmospheric carbon dioxide concentration, *Environ. Res. Lett.*, *8*(3), 34,039, doi:10.1088/1748-9326/8/3/034039.

Cao, L., G. Bala, and K. Caldeira (2011), Why is there a short-term increase in global precipitation in response to diminished CO_2 forcing?, *Geophys. Res. Lett.*, *38*, L06703, doi:10.1029/2011GL046713.

Cao, L., G. Bala, and K. Caldeira (2012), Climate response to changes in atmospheric carbon dioxide and solar irradiance on the time scale of days to weeks, *Environ. Res. Lett.*, *7*(3), 34,015, doi:10.1088/1748-9326/7/3/034015.

Cao, L., G. Bala, M. Zheng, and K. Caldeira (2015), Fast and slow climate responses to CO_2 and solar forcing: A linear multivariate regression model characterizing transient climate change, *J. Geophys. Res. Atmos.*, *120*, 12,037–12,053, doi:10.1002/2014JD022994.Received.

Chadwick, R., I. Boutle, and G. Martin (2013), Spatial patterns of precipitation change in CMIP5: Why the rich do not get richer in the tropics, *J. Clim.*, *26*(11), 3803–3822, doi:10.1175/JCLI-D-12-00543.1.

Chadwick, R., P. Good, T. Andrews, and G. Martin (2014), Surface warming patterns drive tropical rainfall pattern responses to CO_2 forcing on all timescales, *Geophys. Res. Lett.*, *41*, 610–615, doi:10.1002/2013GL058504.

Chou, C., J. D. Neelin, C.-A. Chen, and J.-Y. Tu (2009), Evaluating the "rich-get-richer" mechanism in tropical precipitation change under global warming, *J. Clim.*, *22*(8), 1982–2005, doi:10.1175/2008JCLI2471.1.

Emori, S. (2005), Dynamic and thermodynamic changes in mean and extreme precipitation under changed climate, *Geophys. Res. Lett.*, *32*, L17706, doi:10.1029/2005GL023272.

Fläschner, D., T. Mauritsen, and B. Stevens (2016), Understanding the intermodel spread in global-mean hydrological sensitivity, *J. Clim.*, *29*(2), 801–817, doi:10.1175/JCLI-D-15-0351.1.

Gent, P. R., et al. (2011), The community climate system model version 4, *J. Clim.*, *24*(19), 4973–4991, doi:10.1175/2011JCLI4083.1.

Gregory, J., and M. Webb (2008), Tropospheric adjustment induces a cloud component in CO_2 forcing, *J. Clim.*, *2*, 1–20.

Hansen, J., et al. (2005), Efficacy of climate forcings, *J. Geophys. Res. D Atmos.*, *110*(18), 1–45, doi:10.1029/2005JD005776.

Huang, P. (2013), Regional response of annual-mean tropical rainfall to global warming, *Atmos. Sci. Lett.*, *15*, 103, doi:10.1002/asl2.475.

Kravitz, B., et al. (2013), An energetic perspective on hydrological cycle changes in the Geoengineering Model Intercomparison Project, *J. Geophys. Res. Atmos.*, *118*, 13,087–13,102, doi:10.1002/2013JD020502.

Kvalevåg, M. M., B. H. Samset, and G. Myhre (2013), Hydrological sensitivity to greenhouse gases and aerosols in a global climate model, *Geophys. Res. Lett.*, *40*, 1432–1438, doi:10.1002/grl.50318.

Lambert, F. H., and N. E. Faull (2007), Tropospheric adjustment: The response of two general circulation models to a change in insolation, *Geophys. Res. Lett.*, *34*, L03701, doi:10.1029/2006GL028124.

Martin, G. M., et al. (2011), The HadGEM2 family of Met Office Unified Model climate configurations, *Geosci. Model Dev.*, *4*(3), 723–757, doi:10.5194/gmd-4-723-2011.

Mitchell, B. (1983), The seasonal response of a general circulation model to changes in CO_2, and sea temperatures By, *Q. J. R. Meteorol. Soc.*, *109*(459), 113–152.

Neale, R. B., et al. (2010), Description of the NCAR community atmosphere model (CAM 5.0) *NCAR Tech. Note NCAR/TN-486+ STR*, (April).

O'Gorman, P. a., R. P. Allan, M. P. Byrne, and M. Previdi (2011), Energetic constraints on precipitation under climate change, *Surv. Geophys.*, *33*(3–4), 585–608, doi:10.1007/s10712-011-9159-6.

Pendergrass, A. G., and D. L. Hartmann (2014), The atmospheric energy constraint on global-mean precipitation change, *J. Clim.*, *27*(2), 757–768, doi:10.1175/JCLI-D-13-00163.1.

Previdi, M. (2010), Radiative feedbacks on global precipitation, *Environ. Res. Lett.*, *5*(2), 25,211, doi:10.1088/1748-9326/5/2/025211.

Richardson, T. B., P. M. Forster, T. Andrews, and D. J. Parker (2016), Understanding the rapid precipitation response to CO_2 and aerosol forcing on a regional scale*, *J. Clim.*, *29*(2), 583–594, doi:10.1175/JCLI-D-15-0174.1.

Rugenstein, M. A. A., J. M. Gregory, N. Schaller, J. Sedlacek, and R. Knutti (2016), Oceanic adjustments to radiative forcing, *J. Clim.*, *29*, 5643–5659, doi:10.1175/JCLI-D-16-0312.1.

Samset, B. H., et al. (2013), Black carbon vertical profiles strongly affect its radiative forcing uncertainty, *Atmos. Chem. Phys.*, *13*(5), 2423–2434, doi:10.5194/acp-13-2423-2013.

Samset, B. H., et al. (2016), Fast and slow precipitation responses to individual climate forcers: A PDRMIP multi-model study, *Geophys. Res. Lett.*, *43*, 2782–2791, doi:10.1002/2016GL068064.

Seager, R., N. Naik, and G. A. Vecchi (2010), Thermodynamic and dynamic mechanisms for large-scale changes in the hydrological cycle in response to global warming*, *J. Clim.*, *23*(17), 4651–4668, doi:10.1175/2010JCLI3655.1.

Sherwood, S. C., S. Bony, O. Boucher, C. Bretherton, P. M. Forster, J. M. Gregory, and B. Stevens (2015), Adjustments in the forcing-feedback framework for understanding climate change, *Bull. Am. Meteorol. Soc.*, *96*(2), 217–228, doi:10.1175/BAMS-D-13-00167.1.

Thorpe, L., and T. Andrews (2014), The physical drivers of historical and 21st century global precipitation changes, *Environ. Res. Lett.*, *9*(6), 64,024, doi:10.1088/1748-9326/9/6/064024.

Tian, D., W. Dong, D. Gong, Y. Guo, and S. Yang (2016), Fast responses of climate system to carbon dioxide, aerosols and sulfate aerosols without the mediation of SST in the CMIP5, *Int. J. Climatol.*, doi:10.1002/joc.4763.